PHYSICAL REVIEW B, VOLUME 65, 201402(R)

Characterization of carbon nanotubes using Raman excitation profiles

M. Canonico,[1,2] G. B. Adams,[1] C. Poweleit,[1] J. Menéndez,[1,3] J. B. Page,[1] G. Harris,[2] H. P. van der Meulen,[3] J. M. Calleja,[3] and J. Rubio[3]

[1]*Department of Physics and Astronomy, Arizona State University, P.O. Box 871504, Tempe, Arizona 85287-1504*

[2]*Motorola SPS, DigitalDNA Strategy Office, 2100 East Elliot Road, Tempe, Arizona 85284*

[3]*Departamento de Física de Materiales, C-IV Universidad Autónoma de Madrid, Cantoblanco, Madrid 28049, Spain*

(Received 11 October 2001; revised manuscript received 12 March 2002; published 7 May 2002)

Resonance Raman excitation profiles for several radial-breathing modes in carbon nanotubes have been measured using tunable lasers. It is shown that the *line shapes* of the excitation profiles are a powerful tool for the characterization of the nanotubes. In particular, profiles that follow theoretical predictions for a *single* one-dimensional singularity in the joint density of states can be assigned to armchair tubes. These assignments do not rely on the quantitative details of electronic structure calculations.

DOI: 10.1103/PhysRevB.65.201402 PACS number(s): 73.63.Fg, 78.30.Na

Single-walled carbon nanotubes (CN's) consist of single graphite (graphene) sheets rolled into a tube. Geometrically, there are infinitely many ways in which this can be accomplished. The resulting CN's can be conveniently characterized by two roll-up indices (n,m).[1] It is well known[1] that the CN properties depend on the precise value of n and m, so that a significant effort has been devoted to the development of characterization methods capable of determining these indices. Direct experimental approaches such as electron microscopy[2–4] or scanning probe microscopy[5–7] are very powerful but often impractical, and the need is acute for quick, contactless methods. Optical spectroscopy might be expected to fill this gap. In particular, the CN characteristic vibrational frequencies can be determined with high precision using techniques such as Raman spectroscopy, and the measurements can be compared with calculations based on density functional theory (DFT).[8] The state-of-the-art accuracy of DFT calculations is such that for ordinary systems the underlying structure can be easily identified. CN's, however, are special in that their strongest Raman-active modes are insensitive to the details of their structure. The radial breathing mode (RBM) frequencies ω_{RBM} in these systems depend almost exclusively on the tubes' diameters, and the C-C tangential modes have comparable frequencies for all CN's due to the very similar local carbon environments.[1]

While simple vibrational spectroscopy is unlikely to lead to a complete (n,m) identification, the sensitivity of Raman spectroscopy to the *electronic* structure of the material provides an additional characterization tool. Resonant enhancements in the Raman cross section can be observed when the incident photon energy approaches the energy of interband optical transitions associated with critical points in the joint density of electronic states (JDOS).[9] The optical transition energies can be extracted from an analysis of the resonance excitation profiles (REP's) for Raman-active vibrational modes, and the combination of electronic energies and vibrational frequencies should make it possible to identify the CN's completely.

The resonant nature of Raman scattering in CN's was first demonstrated by Rao *et al.*[10] Following this work, resonance Raman spectroscopy has been frequently used for CN characterization.[11–15] In particular, it has been shown that Stokes/anti-Stokes Raman spectra are dramatically different near resonance,[16,17] and (n,m) assignments have been made based on ω_{RBM} and Stokes/anti-Stokes intensity ratio measurements.[18–21] However, the reliability of such assignments is uncertain, since our current understanding of the electronic structure and the resonance Raman process in CN's is still quite limited. Predicted Stokes/anti-Stokes intensity ratios depend both on the theoretical expressions used for the REPs, as well as on the accuracy of the underlying electronic structure models. Critical parameters in the theoretical REP expressions are the energy separation E_t between the one-dimensional singularities in the valence and conduction bands, and its broadening η, which is related to the lifetime of the virtually excited electron-hole pair. The first parameter is needed for (n,m) assignments via a calculation of the electronic structure, but the second parameter has been shown to affect the predicted Stokes/anti-Stokes ratios considerably.[21]

In this communication we report detailed studies of REPs in CN's using tunable laser sources. These measurements make it possible to determine the transition energy E_t and its broadening η with great accuracy. Moreover, the entire REP line shapes can be compared with theoretical predictions, and we find that these line shapes provide additional characterization information that is largely independent of the details of the electronic structure. Using standard resonance Raman theory, Richter and Subbaswamy[22] have calculated REP's for (n,n) armchair tubes with diameters of practical interest. For these tubes the singularities in the JDOS are separated by more than 1 eV. The calculated REP's are symmetric curves around an energy value close to the JDOS singularity. Calculations for zigzag or chiral CN's are not yet available. However, these tubes present closely spaced singularities (less than 0.3 eV for tube diameters larger than 1 nm) that can be explained in terms of trigonal warping in the graphene band structure.[23] The combined contribution from these singularities is likely to lead to complicated profiles due to their proximity and mutual interference. Therefore, a description of the resonance process in terms of a single, isolated singularity is expected to be valid only for armchair tubes. Our experimental results show that indeed some REP's can be explained in terms of a single one-dimensional (1D) singularity, whereas others show more structure. The former are therefore assigned to armchair tubes.

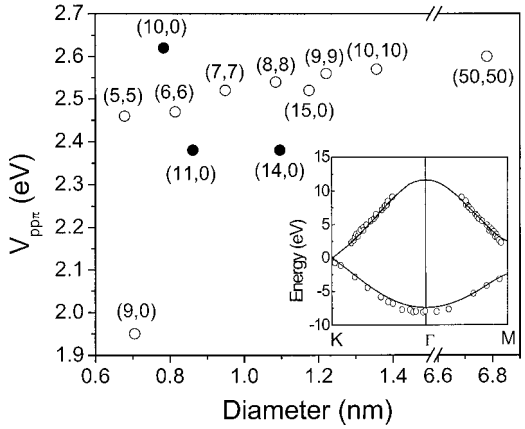

FIG. 1. The inset shows experimental angle resolved photoemission data for graphite (Refs. 27 and 28) compared with a first-principles calculation of the electronic structure of graphene. We used the same first-principles method to calculate the atomic positions and electronic structure of selected nanotubes, and fit the resulting band structures with a simple NNTB model. The solid (empty) circles show our fit values for the parameter $V_{pp\pi}$ for semiconducting (metallic) tubes.

The ability to distinguish armchair from chiral tubes based on the line shape of their REP's is very significant, since (n,m) assignments based solely on ω_{RBM} and E_t values require predictions of interband transition energies with an accuracy that in some cases must exceed 0.1 eV. This is beyond our current understanding of the electronic structure of CN's. Excitonic effects are of the same order of magnitude as the required accuracy,[24,25] and even if these effects are accounted for in an effective way by using empirical band structure models with adjustable parameters, there is no universal agreement as to the value of these parameters. A popular approach for CN's consists of calculating the π-symmetry bands in a graphene sheet using a nearest-neighbor tight-binding (NNTB) model with a single matrix element $V_{pp\pi}$ (also called γ_0 or t in the literature). The 1D CN band structure is then obtained by ''folding'' the graphene band structure in a way that satisfies the CN boundary conditions.[1] The precise value of $V_{pp\pi}$ is controversial, as summarized in Ref. 23. Values ranging from 2.5 to 2.9 eV have been deduced from a variety of experimental techniques.

In Fig. 1 we present theoretical evidence suggesting that the discrepancies between different experimental determinations of $V_{pp\pi}$ may not be entirely due to experimental artifacts. We use the DFT method developed by Sankey and Niklewski[26] as described in Ref. 8. Even though interband transition energies are generally unreliable in DFT, the inset in Fig. 1 shows that our calculated graphene band structure is in very good agreement with the experimental band structure of graphite.[27,28] We have used the same first-principles method, which automatically incorporates effects such as bond relaxation and orbital rehybridization, to calculate the electronic structure of several CN's. We then fit the simple NNTB model to either our calculated band gaps (semiconducting tubes) or to the lowest van Hove singularity in the JDOS (metallic tubes). The results are given by the circles in Fig. 1, and one sees that the first-principles results are not consistent with a single value of $V_{pp\pi}$.

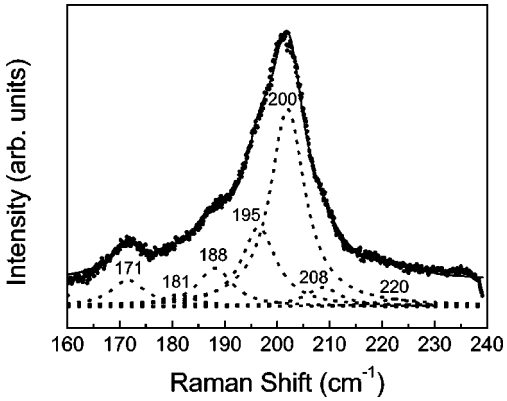

FIG. 2. Typical RBM band from our carbon nanotube sample, obtained with a laser excitation energy of $\hbar\omega_L = 1.989$ eV. The dashed curves represent the Lorentzians needed to fit each spectrum.

Our sample containing single-walled CN's was synthesized by pulsed laser vaporization (PLV) of carbon targets using Ni/Co catalyst particles.[29,30] A transmission-electron-microscopy (TEM) analysis indicates that the mat of carbon ropes contains an ensemble of tube diameters with a mean near 1.25 nm, consistent with previous work on PLV-grown samples.[10,30,31] The material is separated through sonication and then suspended in water with the aid of a surfactant. A drop of the liquid is placed on a silicon substrate and allowed to dry under ambient conditions.

Room temperature Raman spectra were collected in the backscattering geometry using a Spex .85 m double monochromators with charge-coupled device (CCD) detection. The samples were probed with incident energies of 1.879–2.204 eV using Ar-ion pumped dye lasers. The incident power was maintained near 10 mW to prevent sample heating.

Figure 2 shows a typical Raman spectrum in the vicinity of the RBM band. Seven different modes are clearly observed in each spectrum over the excitation energy range. In order to provide consistency in the fitting procedure between spectra, we applied constraints similar to those used by Pimenta *et al.*[12] From the Raman spectra we determined REP's for all modes in Fig. 2 by simply plotting—as a function of the laser photon energy—the peak intensity (area) normalized to the incident power. Some of the measured REP's—such as the ones corresponding to the 195- and 200-cm^{-1} modes in Fig. 3(a)—are smooth curves with a single maximum. Other REP's are clearly more complicated, as seen in Fig. 3(b) for the 188-cm^{-1} mode.

Richter and Subbaswamy[22] find that the dominant contribution to resonant RBM Raman scattering in isolated armchair tubes corresponds to z-polarized optical transitions (z is the axis of the CN) between the ith singularity in the valence band electronic DOS and the ith singularity in the conduction band DOS. The results of Ref. 22 are presented in numerical form, which makes it difficult to fit the theoretical REP's to the experimental data. Fortunately, analytical expressions for REP's near resonance can be derived. If we only include a single critical point arising from 1D parabolic bands, the Raman cross section for an armchair tube is

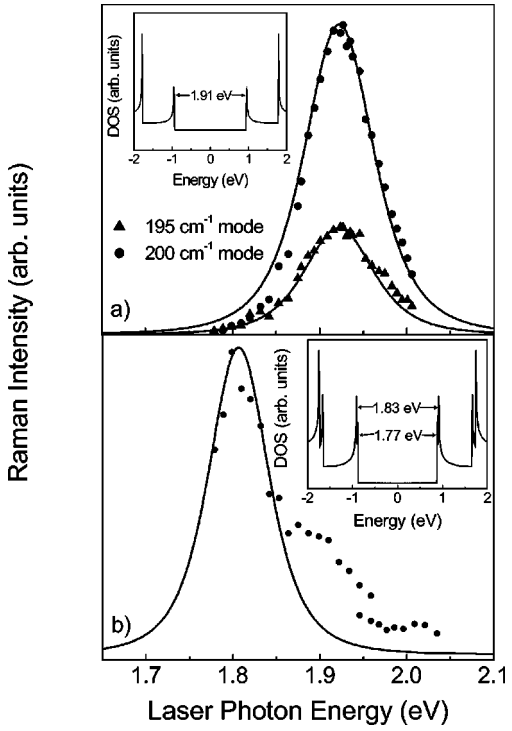

FIG. 3. (a) Raman excitation profiles (REP's) for the 195- and 200-cm^{-1} modes in Fig. 1. The solid lines are fits with an expression proportional to Eq. (1). The inset represents the electronic DOS for a (9,9) tube calculated with the NNTB model using $V_{pp\pi}=2.80$ eV. (b) REP for the 188-cm^{-1} mode in Fig. 1. The solid line is proportional to Eq. (1). It is drawn through the main peak of the resonance to emphasize the deviation between the experimental data and Eq. (1). We used $E_t=1.80$ eV and $\eta=60$ meV. The inset shows the electronic DOS for an (11,8) tube, calculated as discussed in the text.

$$\frac{d\sigma}{d\Omega}=(La)\left(\frac{\omega_S}{\omega_L}\right)^2\left(\frac{eP_z}{mc}\right)^4\left(\frac{m^*}{M}\right)\left(\frac{1}{\hbar\omega_{\mathrm{RBM}}}\right)^3\left|\frac{dE_t}{dR}\right|^2(n+1)$$
$$\times\left|\frac{1}{\sqrt{\hbar\omega_L-E_t-i\eta}}-\frac{1}{\sqrt{\hbar\omega_S-E_t-i\eta}}\right|^2, \qquad (1)$$

where L is the length of the CN, $a=0.246$ nm, ω_S and ω_L are the scattered and incident photon frequencies, e (m) is the electron charge (mass), P_z is the matrix element for the z component of the electronic momentum operator, c is the speed of light in vacuum, m^* is the reduced mass of the virtually excited electron-hole pairs, M is the mass of a carbon atom, n is the phonon population number, and dE_t/dR is the derivative of the transition energy with respect to the radius of the CN. We have verified that this analytical expression provides a very good fit to the numerical results obtained by Richter and Subbaswamy.[22,32] In addition, our expression provides an absolute value (except for possible local field effects) for the Raman cross section, and lends itself to first-principles predictions of Raman intensities via the calculation of dE_t/dR.

At this point we should mention that a nonconventional theory of Raman scattering has recently been used to analyze REP's from single CN's.[18,20] The REP's predicted by this theory are always asymmetric (even for isolated singularities) and are in good agreement with some experimental observations by the same group. However, since asymmetric profiles can also be explained by the conventional theory as a result of interferences and/or superpositions of nearby singularities (or in terms of an interference between the singularity and a nonresonant term which originates from higher-lying optical transitions), we feel that no compelling evidence has been provided to abandon the well-established standard theory of Raman scattering based on the Kramers-Heisenberg formulation.[33]

The solid lines in Fig. 3(a) represent fits with an expression proportional to Eq. (1). From these fits we obtain $E_t=1.91\pm0.01$ eV and $\eta=70\pm5$ meV for the two RBM's. The agreement between the fits and the experimental data is very good, with only a minor hint of deviations from the simple profile described by Eq. (1). By adding a second van Hove singularity to the expression in Eq. (1) we find that interference effects induce noticeable distortions if the two singularities are separated by less than 0.3 eV, whereas the effect is negligible if the separation is much larger. This is consistent with the symmetric profiles computed by Richter and Subbaswamy for armchair tubes,[22] and suggests that interference effects can be important in chiral and zigzag tubes. Thus we assign the REP's in Fig. 3(a) to armchair tubes and the REP in Fig. 3(b) to a chiral or zigzag tube.

So far, we have based our analysis on theoretical results for isolated CN's, whereas the tubes in our samples appear in bundles. Calculations of the electronic density of states for bundles of tubes show that the 1D singularities characteristic of isolated tubes are broadened by at least 0.2 eV.[34,35] The predicted broadenings and distortions might be expected to have an impact on the measured REP's, but our measured broadening $\eta=70\pm5$ meV is significantly smaller than the theoretical predictions. Moreover, our value for η is comparable with direct time-domain measurements of the lifetime of the excited states,[36] suggesting that inhomogeneous broadening does not play an important role in our experiments. A possible explanation for these observations is suggested by a recent comparative study of the electronic structure of crystallinelike and compositionally disordered bundles of CN's.[37] Bundling effects are large when the electronic states become delocalized over the bundle. This is more likely to occur in bundles of *identical* CN's, whereas in heterogeneous bundles the mismatch of the electronic states between nearby tubes leads to wave functions which are essentially localized in individual tubes.[37] Therefore, one might expect REP's obtained from compositionally disordered bundles to be similar to those measured from isolated tubes.

For armchair tubes, the first-principles calculations of Kürti *et al.*[38] predict RBM frequencies of 177 cm^{-1} (10, 10), 195 cm^{-1} (9, 9), and 219 cm^{-1} (8, 8). The theoretical results are supported by the perfect agreement they obtain with the experimental breathing mode frequency in C_{60}. Our experimental RBM frequencies of 195 and 200 cm^{-1} are in good agreement with the theoretical value for (9, 9) tubes, and this is corroborated by TEM studies which show that tubes with the (9, 9) diameter are present in our sample. The small separation between the two experimental frequencies and their nearly identical REP's rule out any assignment to different CN species, so that we assign the two observed modes

to (9, 9) tubes. This is of course quite surprising, because there is only one RBM in an isolated CN. A possible explanation within the context of heterogenous bundles is to assume that the lower-energy mode corresponds to (9, 9) tubes at the surface of the bundle, whereas the 200-cm^{-1} mode corresponds to (9, 9) tubes inside the bundle. In heterogenous bundles the RBM modes are likely to be localized because the RBM frequencies of neighboring tubes do not match exactly, as in the homogenous case. If our interpretation is correct, then the relative intensities in Fig. 3(a) would indicate a surface-to-volume ratio of about 0.38, which corresponds to bundles containing on the order of 100 CN's. This actually agrees with independent measurements of bundle size in these systems[29] and our own TEM results. The 5 cm^{-1} (2.6%) separation between the peaks assigned to the inner and outer tubes represents a lower limit for the upshift induced by bundling, and compares reasonably well with theoretically predicted[39–42] upshifts in the 2.9–10 % range for crystalline ropes. Of course, the observation of virtually identical REP's for the two modes requires that the electronic structure of surface and bulk CN's be very similar. The model presented by Maarouf *et al.* does suggest that intertube interactions can be suppressed in heterogeneous bundles,[37] but it is by no means clear that essentially no electronic energy shifts should be observed, while at the same time the vibrational frequency shifts are on the order of 3%. The clarification of this point will require more experimental and theoretical work.

We now return to the REP of Fig. 3(b). The measured RBM frequency of 188 cm^{-1} is compatible with the rollup indices (11,8), (12,6), (16,1) and (15,3). The inset shows the electronic DOS for an (11, 8) tube calculated with the NNTB model using $V_{pp\pi}=2.80$ eV, which we obtain from a fit to the results of Fig. 3(a). We see that there is some agreement between the calculated transition energies and the peaks in the REP. However, definitive assignments will have to await the development of a quantitative theory of REP's for chiral and zigzag tubes.

In summary, we have studied REP's for the radial breathing modes in CN samples. Our results show that significant progress toward the identification of CN species can be made by studying the line shapes of the REPs within the standard theory of resonance Raman scattering. Our results also suggest that detailed predictions of REP line shapes in chiral and zigzag tubes will make it possible to identify additional CN species. This approach emphasizes the more robust qualitative aspects of the electronic structure of CN's, as opposed to the exact values of their optical transition energies, which we believe are very difficult to predict.

We would like to thank V. Crespi for suggesting the relevance of Ref. 37 for the interpretation of our data. This research was supported in part by NSF under Grant No. INT-0072110. J. M. would like to acknowledge support from the Iberdrola Foundation (Spain) and an International Travel Grant from Arizona State University.

[1] R. Saito, M. S. Dresselhaus, and G. Dresselhaus, *Physical Properties of Carbon Nanotubes* (Imperial College Press, London, 1998).
[2] S. Iijima, Nature (London) **354**, 56 (1991).
[3] S. Iijima and T. Ichihashi, Nature (London) **363**, 603 (1993).
[4] J. M. Cowley *et al.*, Chem. Phys. Lett. **265**, 379 (1997).
[5] M. Ge and K. Sattler, Appl. Phys. Lett. **65**, 2284 (1994).
[6] T. W. Odom, *et al.*, Nature (London) **391**, 62 (1998).
[7] J. W. G. Wildöer *et al.*, Nature (London) **391**, 59 (1998).
[8] J. Menéndez and J. B. Page, in *Light Scattering in Solids VIII: Fullerenes, Semiconduictor Surfaces, Coherent Phonons*, edited by M. Cardona and G. Güntherodt (Springer, Heidelberg, 2000), p. 27.
[9] R. M. Martin and L. M. Falicov, in *Light Scattering in Solids*, edited by M. Cardona (Springer, Berlin, 1975), Vol. 8, p. 79.
[10] A. M. Rao *et al.*, Science **275**, 187 (1997).
[11] M. A. Pimenta *et al.*, Phys. Rev. B **58**, R16016 (1998).
[12] M. A. Pimenta *et al.*, J. Mater. Res. **13**, 2396 (1998).
[13] P. M. Rafailov, H. Jantoljak, and C. Thomsen, Phys. Rev. B **61**, 16179 (2000).
[14] M. Milnera *et al.*, Phys. Rev. Lett. **84**, 1324 (2000).
[15] L. Alvarez *et al.*, Phys. Rev. B **63**, 153401 (2001).
[16] P. Tan *et al.*, Phys. Rev. B **62**, 5186 (2000).
[17] S. D. M. Brown *et al.*, Phys. Rev. B **61**, R5137 (2000).
[18] A. G. Souza Filho *et al.*, Phys. Rev. B **63**, 241404 (2001).
[19] A. Jorio *et al.*, Phys. Rev. Lett. **86**, 1118 (2001).
[20] A. Jorio *et al.*, Phys. Rev. B **63**, 245416 (2001).
[21] Z. Yu and L. Brus, J. Phys. Chem. B **105**, 1123 (2001).
[22] E. Richter and K. R. Subbaswamy, Phys. Rev. Lett. **79**, 2738 (1997).
[23] R. Saito *et al.*, Phys. Rev. B **61**, 2981 (2000).
[24] T. Ando, J. Phys. Soc. Jpn. **66**, 1066 (1997).
[25] M. Ichida, S. Mizuno, Y. Tani *et al.*, J. Phys. Soc. Jpn. **68**, 3131 (1999).
[26] O. F. Sankey and D. J. Niklewski, Phys. Rev. B **40**, 3979 (1989).
[27] A. R. Law *et al.*, Phys. Rev. B **34**, 4289 (1986).
[28] I. Schäfer *et al.*, Phys. Rev. B **35**, 7663 (1987).
[29] A. Thess *et al.*, Science **273**, 483 (1996).
[30] A. G. Rinzler *et al.*, Appl. Phys. A: Mater. Sci. Process. **67**, 29 (1998).
[31] L.-C. Qin and S. Iijima, Chem. Phys. Lett. **269**, 65 (1997).
[32] Richter and Subbaswamy use a broadening parameter of 100 meV, but we obtain 140 meV for this parameter when we fit their calculations with Eq. (2). The most likely reason for this discrepancy is the additional broadening introduced by the numerical treatment of the one-dimensional singularity
[33] H. A. Kramers and W. Heisenberg, Z. Agnew. Phys. **31**, 681 (1925).
[34] J.-C. Charlier *et al.*, Europhys. Lett. **29**, 43 (1995).
[35] Y.-K. Kwon *et al.*, Phys. Rev. B **58**, R13314 (1998).
[36] T. Hertel and G. Moos, Chem. Phys. Lett. **320**, 359 (2000).
[37] A. A. Maarouf *et al.*, Phys. Rev. B **61**, 11156 (2000).
[38] J. Kürti *et al.*, Phys. Rev. B **58**, R8869 (1998).
[39] D. Kahn and J. P. Lu, Phys. Rev. B **60**, 6535 (1999).
[40] U. D. Venkateswaran *et al.*, Phys. Rev. B **59**, 10928 (1999).
[41] L. Henrard *et al.*, Phys. Rev. B **60**, R8521 (1999).
[42] J.-P. Buisson *et al.*, Mater. Res. Soc. Symp. Proc. **633**, A.14.12.1 (2000).